JOURNAL OF SPACECRAFT AND ROCKETS
Vol. 35, No. 1, January–February 1998

Forebody Precompression Effects and Inlet Entry Conditions for Hypersonic Vehicles

Thomas M. Berens* and Norbert C. Bissinger†
Daimler–Benz AG, D-81663 Munich, Germany

To efficiently provide precompressed air to the engine inlets, a hypersonic forebody requires a design with potentially contradictory optimization goals: a high static pressure for the inlet entry flow and a large air mass flow to reduce engine size and hence vehicle drag, the maximization of the total kinetic energy for the inlet air, and a small Mach number and flow distortion across the inlet face to guarantee the undisturbed operation of inlets and engines. Starting with basic elliptic, flat, and concave cross sections of the forebody's bottom side, 11 sharp-nosed, hypersonic-flight-test-vehicle-type forebodies of varying cross-sectional shapes were designed for a numerical investigation of their influence on propulsion and aerodynamic performance. Three-dimensional Euler calculations were carried out for flight Mach numbers 3.5 and 6.8 at angles of attack of 0 and 6 deg. Slim narrow forebodies provide the highest air mass flow rates for the engines and result in the lowest total pressure losses for the inlet entry area. Their external aerodynamic behavior is characterized by low drag and large lift components. Elliptical and concave cross-sectional shapes of the forebody's bottom side are preferable to flat geometries.

Nomenclature

A	= area, m^2
c_D	= drag coefficient, $D/q_\infty A_{\text{ref}}$
c_L	= lift coefficient, $L/q_\infty A_{\text{ref}}$
c_m	= moment coefficient, $M/q_\infty A_{\text{ref}} l_{\text{ref}}$
$c_{\dot{m}d}$	= mass-flow-to-drag ratio, $A_\infty/A_0 c_D$
D	= drag, N
L	= lift, N
l	= fuselage length, m
M	= moment, Nm
Ma	= Mach number
$\dot{m}$	= mass flow, kg/s
p	= pressure, Pa
q_∞	= freestream dynamic pressure, $0.5\rho_\infty v_\infty^2$, Pa
v	= velocity, m/s
α	= angle of attack, deg
ρ	= density, kg/m^3

Subscripts

ref	= reference value
s	= static state
t	= total state
x, y, z	= coordinates
0	= inlet entry state
∞	= ambient condition

Introduction

THE design and integration of the forebody of a hypersonic vehicle require intensive research because the forebody's geometry greatly influences the overall performance of the vehicle.[1–4] In providing precompressed air to the engine's inlets, the forebody plays a vital role in achieving high propulsion efficiency. According to the vehicle's mission, requirements on adequate lift and limited drag must be met. To avoid spillage mass flow and hence to reduce drag, the compression shock created by the nose of the forebody should impinge on the inlet cowl's lip at the design point for optimum performance.

From a propulsion point of view, design goals for the forebody include a high static pressure at the inlet face and a large inlet air mass flow, i.e., a large area ratio of the captured stream tube. Propulsion efficiency also requires the maximization of total kinetic energy at the inlet entry or, in other words, the minimization of total pressure losses; a small Mach number at the inlet face is desirable. Furthermore, the optimization of the flow quality for an efficient engine operation comprises small gradients of all flow parameters and a minimized distortion (small local angles of attack and local angles of yaw) across the inlet face. When the equally important external aerodynamic performance of the forebody's shape is included, such parameters as the lift-to-drag ratio and the moment coefficient for longitudinal stability broaden the complexity of the design process for hypersonic forebodies. For the vehicle to perform a successful mission, all of the aforementioned parameters, as well as issues concerning structures, heat transfer, and volume for onboard equipment, must be considered when developing the vehicle's forebody.[5] The optimization of a hypersonic propulsion system requires the harmonization of all individual components[6,7] to gain maximum efficiency and thus to meet challenging technology demands.

The work presented in this paper deals with the three-dimensional flowfields around various forebody shapes for the type of hypersonic experimental aircraft with a highly integrated propulsion system[8,9] shown in Fig. 1. Numerically obtained data for propulsion- and aerodynamics-related design parameters are provided for flight Mach numbers 3.5 and 6.8 at angles of attack of 0 and 6 deg. The precompression data set enables the consideration of the aerodynamic interaction between the forebody and the inlets in an early phase of the vehicle design process.

Forebody Geometry

Forebody precompression of the airflow is influenced by a great number of geometrical parameters. A strong effect on the three-dimensional flowfield is given by the cross-sectional shape of the forebody's bottom side[1] (elliptical, flat, or concave) and the lateral extension (wide or narrow body). Other important geometrical features are the transition from the bottom side to the side wall with sharp or rounded edges in various styles, the relative position of the vehicle's nose and its shape (pointed, rounded), and the forebody's length and longitudinal cross section (slim, blunt). For fuselage geometries with a height-to-width ratio on the order of one (see Fig. 1), which are of special interest here, three-dimensional effects are most important, and the vast variety of possible geometrical modifications enlarges the complexity of the forebody design.

Presented as Paper 96-4531 at the AIAA 7th Annual International Spaceplanes and Hypersonic Systems and Technologies Conference, Norfolk, VA, Nov. 18–22, 1996; received Feb. 20, 1997; revision received May 30, 1997; accepted for publication June 3, 1997.

*Aerospace Research Engineer, Propulsion Intake/Afterbody Department, Military Aircraft Division. Senior Member AIAA.

†Group Leader, Intake/Afterbodies, Propulsion Intake/Afterbody Department, Military Aircraft Division.

For a numerical investigation of the three-dimensional flowfield around forebody shapes with special emphasis on precompression effects and inlet entry conditions, 11 sharp-nosed, hypersonic-flight-test-vehicle-type forebodies were designed with the computer-aided three-dimensional interactive application (CATIA). Starting with a slim fuselage configuration and basic elliptic, flat, and concave cross-section types of the forebody's bottom side, for each of these three categories different design variations and modifications with reference to cross-sectional shaping, width, and bluntness of the forebody were carried out. Figure 2 gives an overview of all forebody modifications investigated in this study. For identification purposes a code of five letters was established that characterizes the specific forebody design. The first letter in all cases is F and is a reference for forebody. The second letter describes the basic cross-sectional shape of the forebody's bottom side: E for elliptic, F for flat, and C for concave. The longitudinal cross section in the symmetry plane of the vehicle is denoted by the third letter: S for slim and B for blunt. The fourth letter characterizes the top view of the forebody geometry: N for narrow and W for wide. The special design variation of the basic cross-sectional type is given by the fifth letter. As an example, the identification code FFSWB describes a forebody (F) with a flat (F) bottom side, a slim (S) design for the longitudinal cross section in the fuselage's symmetry plane, a wide (W) layout viewed from the top, and a certain variation (B) of the flat cross-sectional shape of the bottom side (compare Fig. 2).

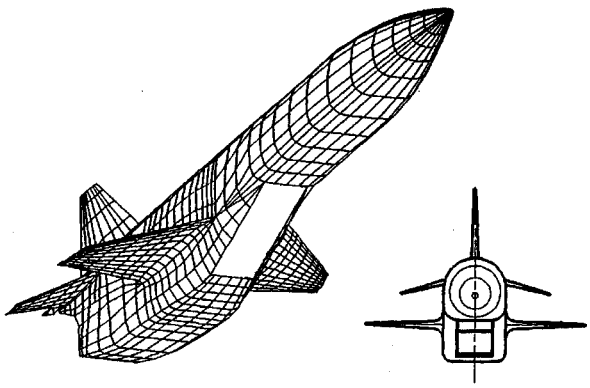

Fig. 1 Hypersonic experimental aircraft.[8,9]

All geometry variations have the same length, the same position of the pointed nose tip, and also the same cross section for the joining edge to the middle part of the fuselage. The forebody length of 4260 mm and the size of the fuselage joining edge are compatible with possible hypersonic flight test vehicles of the category shown in Fig. 1. The distance between the vertical projection of the nose tip on the joining edge cross section and the bottom side of the forebody measures one-third of the joining edge's height (see Fig. 2). The cross-sectional shape for each forebody (elliptic, flat, or concave) was prescribed at one-third of the overall forebody length and

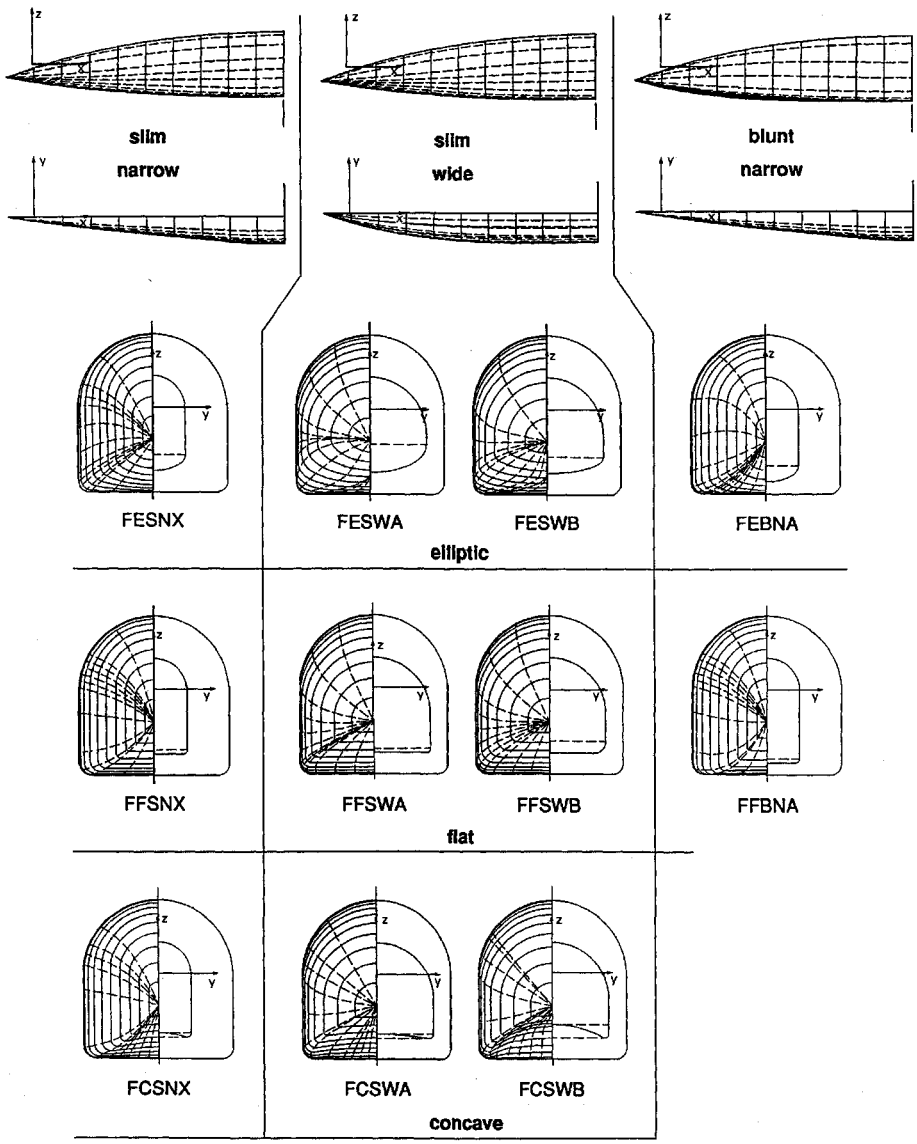

Fig. 2 Overview of all forebody modifications under investigation.

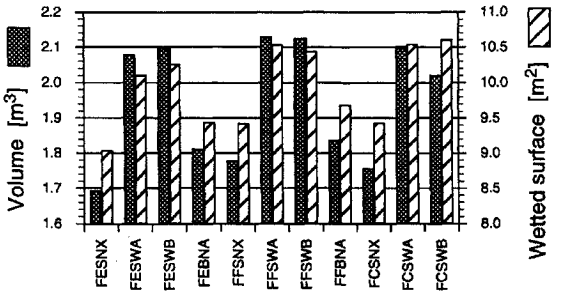

Fig. 3 Volumes and wetted surfaces of the different forebody variations.

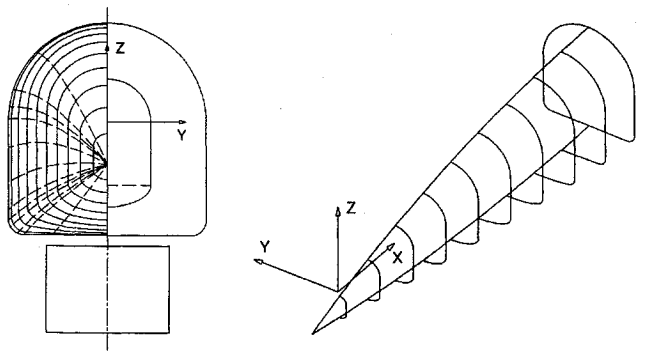

Fig. 4 Front view and three-dimensional view of the forebody FESNX with the inlet capture area.

was used to create the surface geometry from the nose tip to the joining edge of the fuselage. All narrow forebodies possess the same top side geometry. Also, for all wide designs, the forebodies' top sides remained unchanged. Figure 3 shows the volumes and wetted surfaces of the designed forebody variations (complete forebodies). The values for the surfaces do not contain the cross section for the joining edge, which has an overall size of 0.8172 m^2.

Figure 4 shows the front view of the forebody FESNX and a three-dimensional view with cross sections 426 mm apart (one-tenth of the body's length) as an example for the CATIA geometry. The left-hand side of the front view (see also Fig. 2) illustrates the generated surface of the forebody with the specified cross-sectional shapes (solid lines) and some CATIA system-defined surface lines (dashed lines). The front view's right-hand side contains the prescribed cross-sectional shape at one-third of the overall forebody length for the generation of the forebody surface and shows the contour of the joining edge to the middle part of the fuselage. The dimensions of the inlet face (height 404 mm and width 571 mm) in front of the inlet's first ramp are also shown with the forebody's front view. A diverter height of 50 mm was taken into account during the evaluation of the precompression data.

Computational Fluid Dynamics Model

For the forebody modifications, surface grids were generated that were used to create the space grids for the Euler calculations. The surface grid on a forebody's half model consists of 59 grid lines in the longitudinal direction, 25 grid lines in the lateral direction on the upper and bottom sides, and 33 grid lines on the body's side wall. To meet computational requirements for the numerical scheme, the density of the grid lines is higher in the vicinity of the walls and toward both ends of the body than in the outer flowfield. The size of the computational domain was adjusted to the hypersonic flow conditions and has a trapezoidal shape in the side view and in the view from the top. The height and the width of the domain's boundary in the plane of the forebody's joining edge were chosen in such a way that the shocks that are generated at the tip of the forebody will leave the computational domain through this boundary for all investigated combinations of flight Mach numbers and angles of attack. The space grid was established with 69 × 50 × 76 grid lines in the x, y, and z directions (for the coordinate system, see Fig. 4), leading to 262,200 nodal points. All numerical results documented in this paper were obtained by using the same grid structure. To investigate the influence of the grid density on the numerical data, a space grid with 970,200 nodal points (105 × 77 × 120 grid lines) was generated for the forebody FESNX within the same computational domain, and a calculation was carried out for a selected test case ($Ma_\infty = 3.5$ and $\alpha = 6$ deg). Deviations of the numerical results were within the range of 0.3%. For analysis of the three-dimensional flowfield around the forebody geometries, the DASA-EUFLEX (Euler code with characteristic flux extrapolation) computer code with a cell-centered finite volume scheme was used.[10,11]

Precompression Data Set

The static pressure ratio, the Mach number, the stream tube total pressure ratio, and the stream tube area ratio (mass flow) describe the inlet entry conditions and decisively affect inlet design. Values of these parameters are presented for all forebody geometries and the investigated flight envelope. Unfortunately, because of budget cuts no calculations at $\alpha = 0$ deg could be carried out for FCSWB, so that the performance of this forebody could not be evaluated completely.

Static Pressure Ratio

At $Ma_\infty = 3.5$, narrow forebodies produce high static pressure ratios across the inlet face for the investigated angle-of-attack range independent of the cross-sectional shapes of their bottom sides (Fig. 5). Among the wide forebodies, a geometry with a strongly curved concave cross section (FCSWB) is advantageous compared with elliptical and flat geometries with respect to static pressures. For $\alpha = 0$ deg, elliptical and concave geometries with a narrow body produce the same static pressures across the inlet area. For the investigated scope of angles of attack, blunt geometries are in midrange.

At $Ma_\infty = 6.8$ and high angles of attack, wide forebodies lead to highest pressures, whereby geometries with concave bottom sides rank at the top, followed by elliptical shapes. At 0-deg angle of attack, slight advantages are gained by narrow forebodies, but concave cross sections are also superior. For a flight Mach number of 6.8, the lowest static pressures are delivered by blunt geometries, whereby the body with the flat contour of the bottom side (FFBNA) ends up last.

Inlet Entry Mach Number

Figure 6 shows that, in accordance with static pressure ratios, low inlet entry Mach numbers are achieved by narrow forebodies at $Ma_\infty = 3.5$. Wide bodies with emphasized concave contours deliver even lower values for M_0. Other than this, wide bodies are responsible for high inlet entry Mach numbers; the highest values are produced by forebodies with flat bottom sides.

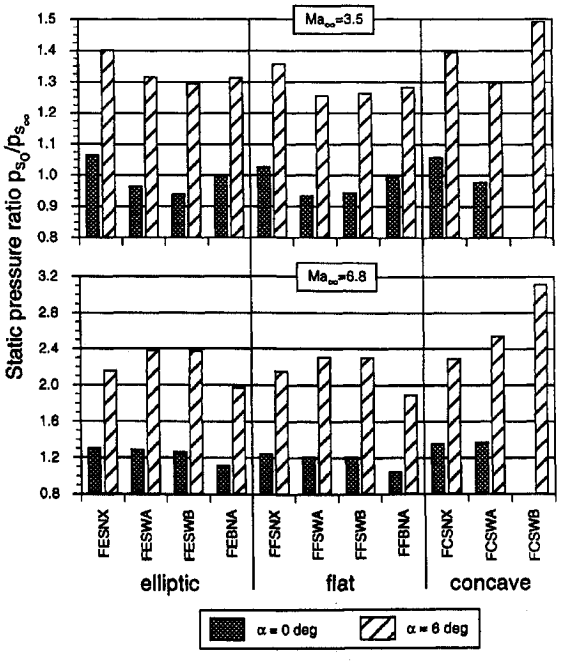

Fig. 5 Static pressure ratios.

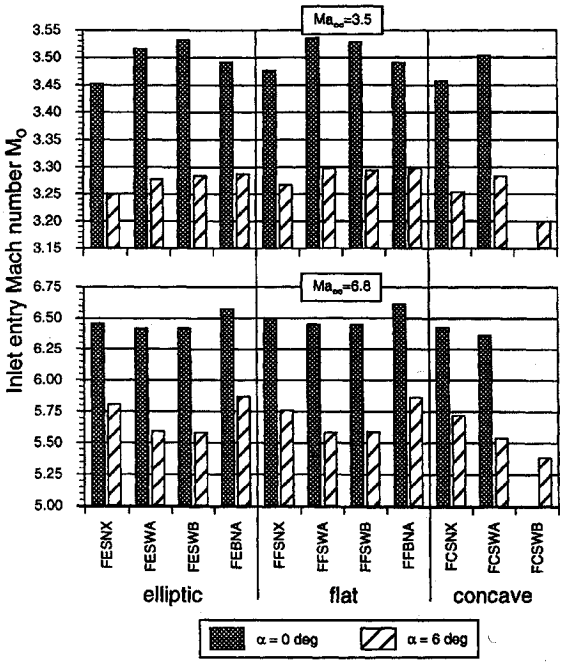

Fig. 6 Inlet entry Mach numbers.

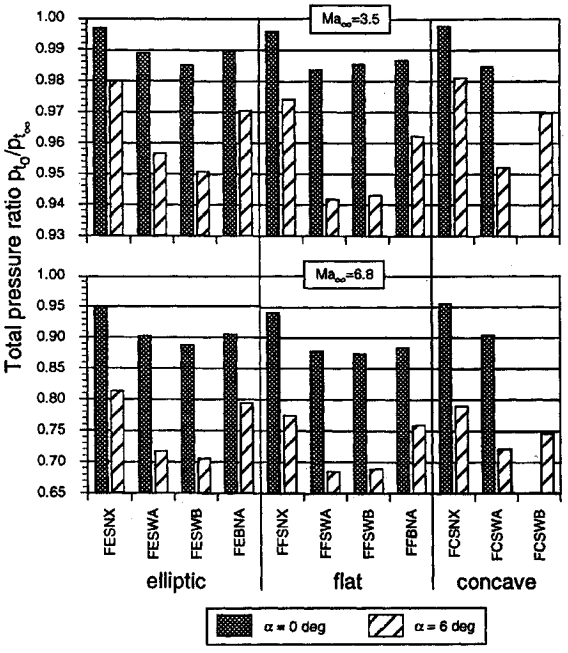

Fig. 7 Total pressure ratios.

For $Ma_\infty = 6.8$ and $\alpha = 0$ deg, all forebodies show similar inlet entry Mach numbers. Because of stronger expansion of the air along the blunt body shapes, the Mach numbers for FEBNA and FFBNA reach highest values. Increasing the angle of attack at $Ma_\infty = 6.8$ results in greater differences for the forebodies in question. Here, wide geometries lead to the lowest Mach numbers across the inlet face with no preference for a certain cross-sectional bottom shape. As expected, blunt geometries come out badly at both angles of attack.

Total Pressure Ratio

As Fig. 7 reveals, the lowest total pressure losses (the highest total pressure ratios) within the stream tube captured by the inlet are gained by narrow forebodies for the complete Ma_∞/α spectrum investigated. For small angles of attack, the shape of the bodies' bottom sides plays a minor role. For an angle of attack of 6 deg, forebodies with elliptical and concave contours are superior. The worst values for the total pressure ratio are delivered by wide forebodies with flat bottom sides for all Mach numbers and angles of attack under consideration. In general, differences for pressure recovery appear smaller at $\alpha = 0$ deg than for high angles of attack, where different geometries show greater effects, especially at low Mach numbers.

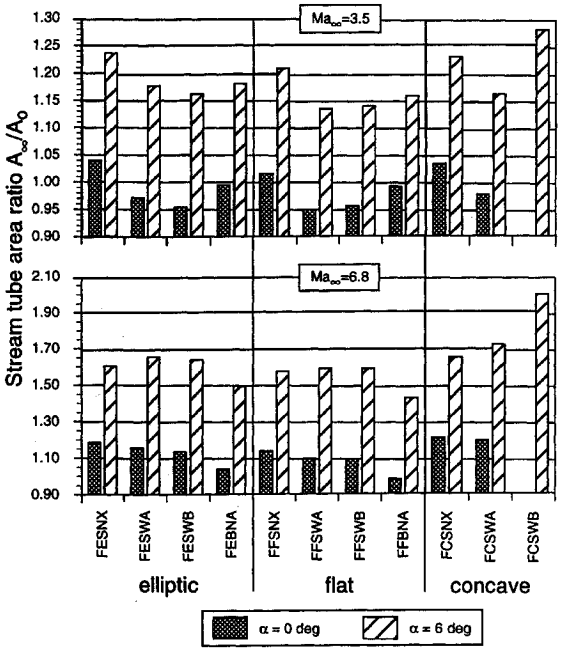

Fig. 8 Stream tube area ratios.

Stream Tube Area Ratio (Inlet Mass Flow)

The area ratios of the stream tube captured by the inlet, which is a measure for the engine mass flow, are documented in Fig. 8. The highest values are present for the slim narrow forebody geometries at $Ma_\infty = 3.5$. A very good performance within the complete angle-of-attack range is achieved by elliptical and concave shapes of the bottom side. The wide forebody with the concave contour (FCSWB) gives the best value for the area ratio. Among the wide bodies, elliptical and concave shapes prove to be beneficial compared with flat geometries. Blunt bodies deliver comparatively good values for the inlet air mass flow at $Ma_\infty = 3.5$ but perform poorly at $Ma_\infty = 6.8$. Furthermore, at $Ma_\infty = 6.8$ and $\alpha = 6$ deg, wide bodies are preferable. Their advantage over narrow geometries is not prominent, with the exception of the configuration with a strongly contoured concave bottom side (FCSWB), which provides the greatest mass flow for the inlet. At small angles of attack, slim narrow geometries are superior to wide bodies, and the bottom side's shape is of minor importance.

Isolines

Requirements on forebody aerodynamics are a most homogeneous flow at the inlet face with smallest possible gradients of the relevant flow parameters (Mach number, pressure, and flow angles) to guarantee an undisturbed inlet operation and hence a reliable engine performance. The overall goal of improving the flow quality is the minimization of the inlet capture area and hence the reduction of inlet drag. At the same time, the achievement of the best possible inlet performance is desired.

To characterize the flow state in the inlet entry plane in front of the first inlet ramp (fuselage joining edge cross section), lines of constant static pressure ratios at $Ma_\infty = 3.5$ and $\alpha = 6$ deg are shown in Fig. 9 for a selection of forebodies with an elliptical cross section of their bottom sides. Figure 4 gives the size of the inlet face at the inlet entry plane for which the flow state is of major interest. For narrow forebodies (FESNX and FEBNA; Fig. 2) large gradients of all flow parameters are generally present at the side walls. Because of increased flow expansion, these gradients are less distinct for blunt bodies (FEBNA). Also as a result of flow expansion at the front part of the fuselage, wide bodies (FESWA and FESWB) produce a flowfield in the inlet plane with an extended area of change for the flow state in the lateral direction. Increasing the angle of attack generally results in an intensified flow in the lateral direction and

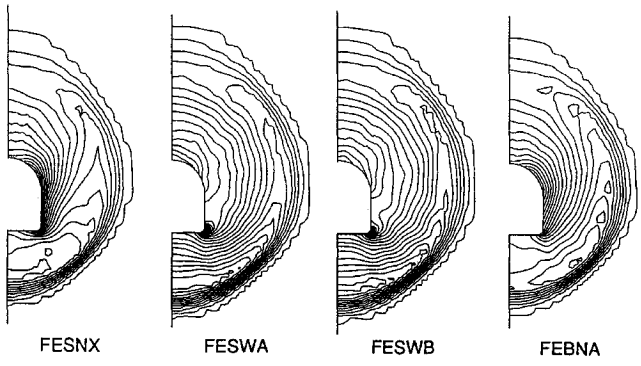

Fig. 9 Lines of constant static pressure ratios (increment 0.05).

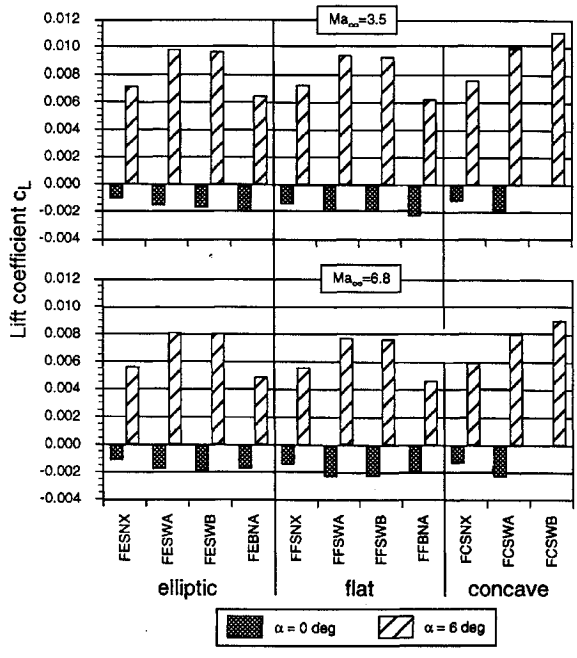

Fig. 10 Lift coefficients.

hence around the bottom edge (transition from bottom to side walls) with large gradients of the flow parameters close to the forebody walls in this area. The inlet face, however, remains untouched by these strong changes of state. Changes in the local angles of attack and the local angles of yaw across the inlet face are relatively small. Flow patterns for the investigated forebodies with flat and concave contours are similar in their character. For all investigated forebodies and flight conditions, a relatively homogeneous flowfield is present within the inlet entry area. Gradients for the flow parameters increase slightly with increasing Mach numbers and increasing angles of attack. With increasing flight Mach numbers, the forebody front shock moves closer to the body and at $Ma_\infty = 6.8$ might interact with the inlet lip. For an extended analysis of the shock location in this region, a refinement of the computational grid is required.

Aerodynamic Coefficients

Concerning external aerodynamics, the optimization of the forebody's aerodynamic shape is governed by the maximization of the lift-to-drag ratio and the minimization of drag. Longitudinal and lateral stability of the vehicle are vital boundary conditions for flight mechanics. For an enhanced assessment of the performance of the forebody modifications, lift, drag, and moment coefficients were calculated, as well as parameters derived from these numbers. The coefficients are based on the following reference values: 22.0 m^2 for the vehicle's projection area A_{ref} and 12,100 mm for the fuselage length l_{ref}. The coordinates for the vehicle's center of gravity were assumed at $x = 6700$ mm, $y = 0$ mm, and $z = -150$ mm. (The coordinates for the forebody tip are $x = -400$ mm, $y = 0$ mm, and $z = -200$ mm; see Fig. 4.) The coefficients are defined in the nomenclature and are valid for the complete models of the forebodies.

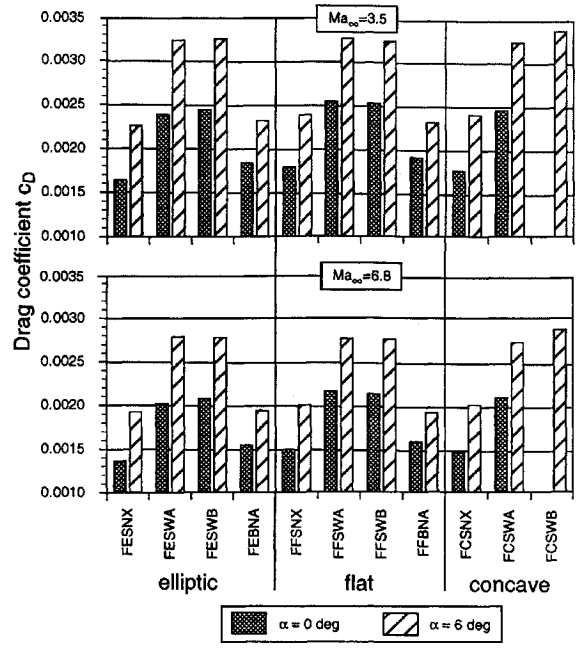

Fig. 11 Drag coefficients.

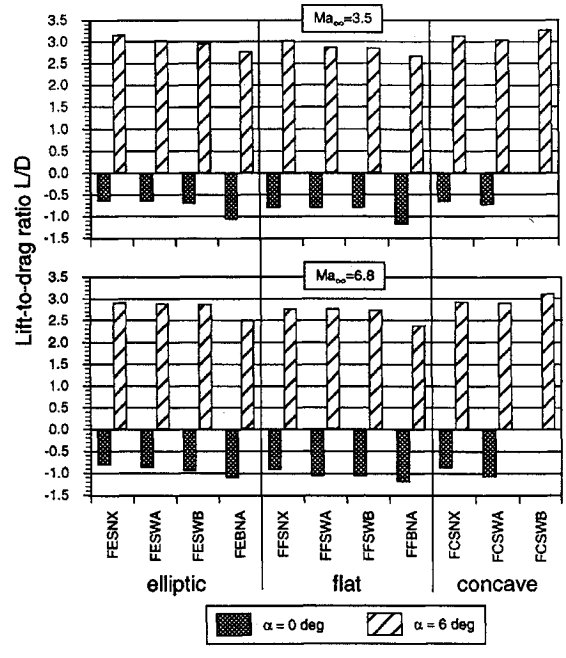

Fig. 12 Lift-to-drag ratios.

Because of a design for an operation up to an angle of attack of 9 deg, all forebody modifications show negative lift at 0-deg angle of attack (Fig. 10). Naturally, absolute values are larger for wide bodies than for narrow geometries. Narrow blunt forebodies also show comparatively large negative lift as a result of the strong expansion on the bottom side and corresponding low pressures. At $\alpha = 6$ deg, best lift coefficients are achieved by wide bodies; only minor differences are present between the geometries with different contours of the bottom side (elliptical, flat, or concave).

A comparison of the drag coefficients (Fig. 11) reveals large values for the voluminous geometries (see Fig. 3). The influence of the bottom side shapes is not prominent. For both investigated Mach numbers, the wide body with a strongly curved concave cross section (FCSWB) produces the largest drag.

As a result of negative lift, the lift-to-drag ratio (Fig. 12) cannot be used for comparison of the forebodies' external aerodynamic

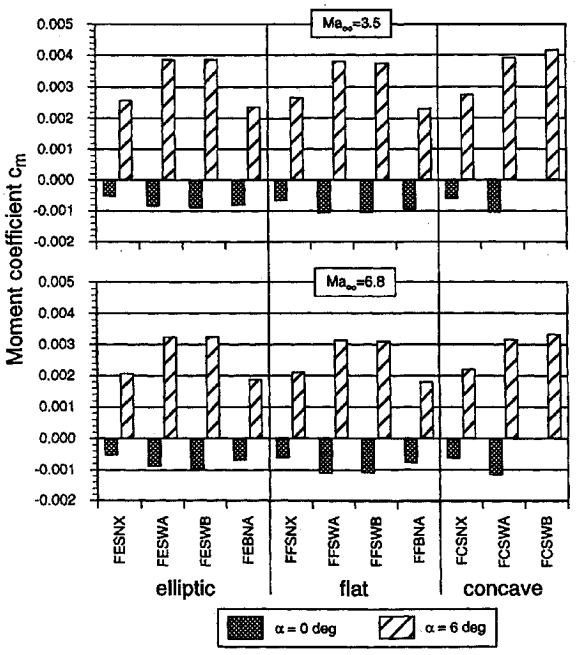

Fig. 13 Moment coefficients.

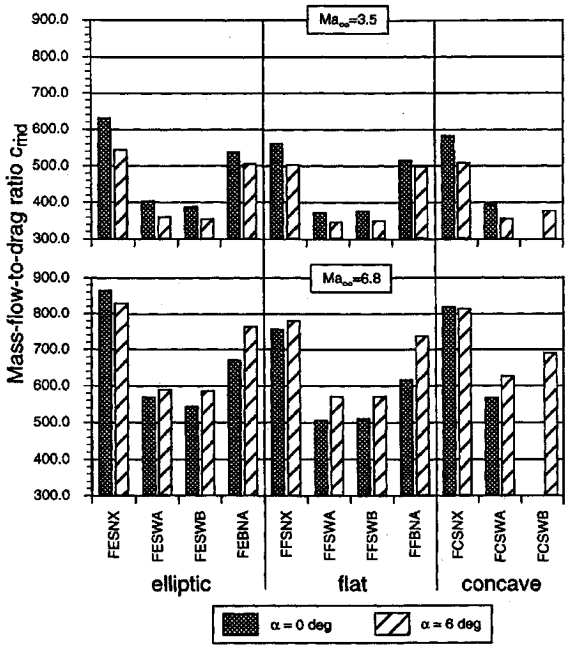

Fig. 14 Mass-flow-to-drag ratios.

performance for $\alpha = 0$ deg. For $\alpha = 6$ deg, forebodies with concave contours have the highest lift-to-drag ratios, whereby the advantage over other configurations is not pronounced. Forebodies with elliptical bottom sides come out somewhat better over flat shapes.

Concerning the longitudinal stability, the moment coefficients (Fig. 13) are negative for $\alpha = 0$ deg, showing the same trend as the lift coefficients. For high angles of attack, all forebodies produce nose-up moments.

In forebody performance evaluation, an interesting parameter is the mass-flow-to-drag ratio (Fig. 14), which combines propulsion criteria with external aerodynamic requirements.[3] As an equivalent parameter for the inlet air mass flow, the area ratio of the captured stream tube was used. If the primary goal with forebody optimization is the maximization of inlet air mass flow with simultaneously minimized drag, narrow forebodies are promising candidates. Even blunt body configurations are advantageous in this respect. Elliptical and concave shapes of the bottom side are preferable to flat contours. In these considerations, the angle of attack plays a minor role, although its influence cannot be neglected for specific cases.

Conclusions

Hypersonic vehicles require highly integrated forebodies to utilize precompression effects and to contribute to an overall efficient propulsion system. The design of the forebody shape strongly depends on the vehicle flight path (Mach number and angle of attack) and is influenced by a great number of optimization goals. Demands from the propulsion system (high static and total pressures, low Mach number, large air mass flow, and small flow distortion at the inlet entry face), as well as requirements from external aerodynamics (high lift, low drag, and stability), lead to a highly complex design process. Furthermore, structural strength, heat transfer, and the necessary volume for equipment and payload must be considered.

For a numerical investigation of forebody precompression effects, 11 sharp-nosed geometries with elliptic, flat, and concave cross-sectional shapes were designed. Three-dimensional Euler calculations were carried out for flight Mach numbers 3.5 and 6.8 at angles of attack of 0 and 6 deg. To describe the inlet entry conditions, which decisively affect inlet design, the static and total pressure ratios for the captured stream tubes, the inlet entry Mach numbers, and the stream tube area ratios were calculated. To include aerodynamic performance in the forebody assessment, lift, drag, and moment coefficients, as well as parameters derived from them, were also calculated.

From the perspective of inlet performance, slim narrow forebodies are generally the most attractive because they deliver the largest values for the stream tube area ratio and hence the inlet air mass flow for the flight envelope under consideration and result in the lowest total pressure losses for the inlet entry area. Inlet entry Mach numbers for slim narrow forebodies lie at the lower end of the scope at $Ma_\infty = 3.5$ for all angles of attack and in comparison are still fairly small for high Mach numbers, although they fail to achieve lowest (best) values. In accordance with inlet entry Mach numbers, values for the static pressure ratio are best for slim narrow forebodies at low Mach numbers and average at $Ma_\infty = 6.8$ and $\alpha = 6$ deg. Considering external aerodynamic behavior, their preferred application is furthermore underlined by excellent performance ranks. At minimized drag and with large lift components, high air mass flow rates are provided for the engine. Thus, slim narrow forebodies best fulfill requirements of both the propulsion system and external aerodynamics. Wide bodies with strongly curved, concave cross sections of the bottom side exhibit excellent performance for high angles of attack (small inlet entry Mach numbers, high static pressure ratios for the inlet captured stream tube, large inlet air mass flow rates, and best lift-to-drag ratios) and hence possess a large application potential, too. Although top performance cannot be achieved with respect to total pressure by this body, losses are fair, especially in comparison with all other wide bodies. Concerning cross-sectional shapes of the forebody's bottom side, elliptical and concave contours are preferable to flat geometries because the flow parameters affecting inlet design, the flow quality at the inlet face, and the aerodynamic coefficients come out better.

For all of the designed forebody modifications and the investigated flight envelope, only small gradients of the flow parameters are present within the inlet entry area. Because of this small distortion in the flowfield, disturbances in the inlet operation are not to be expected. At $Ma_\infty = 6.8$ and $\alpha = 6$ deg, the forebody front shock lies in the close vicinity of the inlet lip. Refinement of the computational grid would lead to a proper analysis of the flow phenomena in this region. For further evaluation of the three-dimensional flowfields around the forebodies, viscous aspects of the flow, e.g., boundary-layer growth and behavior, must be taken into consideration.

Because the operational requirements of a hypersonic vehicle for external aerodynamic behavior and the demands from the propulsion system are strongly flight mission dependent, the forebody geometry must be tailored to the individual performance needs of a certain aircraft. Also, to optimize the performance of the complete propulsion system, the aerodynamic interaction between the forebody and

the inlets must be considered. Both components have to be adapted to each other to meet the highest technology demands. In this design process, computational fluid dynamics has proven to be a valuable tool to approach sensitivities of various forebody design parameters and to explore the precompression efficiency and the aerodynamic performance at an early phase of the vehicle design process.

Acknowledgments

This work was part of the study "Hypersonic Technology Program: Intake" (Daimler–Benz Aerospace AG, Dasa-LMLE3-HYPAC-STY-0018-A, Munich, Germany, October 1996) funded by the German Ministry of Research and Technology. The support of P. W. Sacher, Project Manager at Dasa's Military Aircraft Division, for all hypersonic activities, is greatly appreciated. The authors gratefully acknowledge the supporting interest of their colleagues in the Propulsion Intake/Afterbody Department.

References

[1]Ide, H., Armstrong, J., Szema, K. Y., and Haney, J., "Hypersonic Vehicle Forebody Design Studies and Aerodynamic Trends," AIAA Paper 89-2182, July/Aug. 1989.

[2]Newberry, C. F., Dresser, H. S., Byerly, J. W., and Riba, W. T., "The Evaluation of Forebody Compression at Hypersonic Mach Numbers," AIAA Paper 88-0479, Jan. 1988.

[3]Wilson, G. J., and Davis, W. H., "Hypersonic Forebody Performance Sensitivities Based on 3D Equilibrium Navier–Stokes Calculations," AIAA Paper 88-0370, Jan. 1988.

[4]Sommerfield, D., Dao, S. C., Schwartz, M., and Wai, J. C., "Hypersonic CFD Analysis of Generic Forebodies," AIAA Paper 88-0372, Jan. 1988.

[5]Hirschel, E. H., "Aerothermodynamic Phenomena and the Design of Atmospheric Hypersonic Airplanes," *Advances in Hypersonics*, 1st ed., Vol.1, Birhäuser, Basel, Switzerland, 1993, pp. 1–39.

[6]Berens, T., "Antriebsintegration und Aerothermodynamik," Abschlussbericht, Daimler-Benz Aerospace AG, Dasa-LME12-HYPAC-STY-0016-03-A, Munich, Germany, Sept. 1995.

[7]Berens, T., "Thrust Vector Optimization for Hypersonic Vehicles in the Transonic Mach Number Regime," AIAA Paper 93-5060, Nov./Dec. 1993.

[8]Sacher, P. W., "Flight Testing Vehicles for Verification and Validation of Hypersonics Technology," AGARD Symposium on Space Systems Design and Development Testing, Paper No. 23, Oct. 1994.

[9]Sacher, P. W., "Hypersonic Flight Testing Issues," AIAA Paper 93-5078, Nov./Dec. 1993.

[10]Heiss, S., Eberle, A., Fornasier, L., and Paul, W., "Application of the Euler Method EUFLEX to a Fighter-Type Airplane Configuration at Transonic Speed," AIAA Paper 92-2620, June 1992.

[11]Eberle, A., Schmatz, M. A., and Bissinger, N. C., "Generalized Flux Vectors for Hypersonic Shock-Capturing," AIAA Paper 90-0390, Jan. 1990.

J. R. Maus
Associate Editor